Analyst

Accepted Manuscript

This article can be cited before page numbers have been issued, to do this please use: R. Ayyanu and P. Perumal, *Analyst*, 2018, DOI: 10.1039/C8AN00377G.

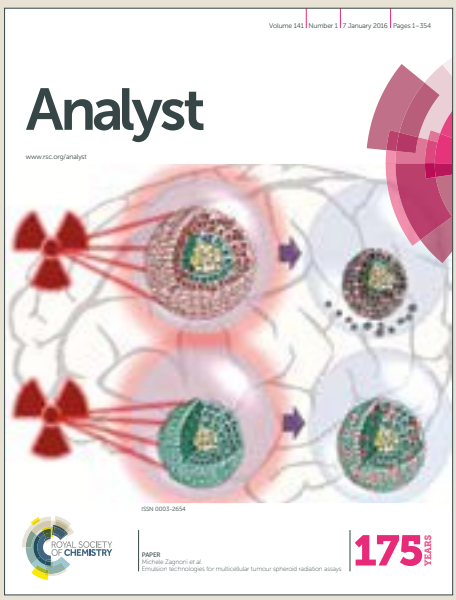

ROYAL SOCIETY OF CHEMISTRY

rsc.li/analyst

View Article Online
DOI: 10.1039/C8AN00377G

Polydopamine Nanotubes mediated Fluorescent Biosensor for Hg(II) Determination through Exonuclease III-Assisted Signal Amplification

A. Ravikumar, P. Panneerselvam*

Department of Chemistry, SRM Institute of Science and Technology, Kattankulathur-603 203, Tamil Nadu, India.

* Corresponding author & E-mail address: panneerselvam.pe@ktr.srmuniv.ac.in

panneerchem82@gmail.comTel: +91 9688538842

View Article Online
DOI: 10.1039/C8AN00377G

Abstract

We describe a highly sensitive fluorescence biosensor for the determination of Hg^{2+} in aqueous solution which has been developed by polydopamine nanotubes (PDNTs). It is based on the mechanism of exonuclease III (Exo III) assisted signal amplification. The fluorescent probes of FAM labeled ssDNA (FAM-ssDNA) adsorbed on PDNTs are efficient quencher. In presence of Hg^{2+}, the FAM-ssDNA can bind Hg^{2+} to form double strand DNA (dsDNA) via T-Hg^{2+}-T base pairs was formed. Then, dsDNA were removed from the PDNTs surface and hence restores the fluorescence. The released dsDNA was triggered by Exo III digestion. At the same time, the liberated Hg^{2+} mediates a new cycle of digestion. This assay is ultrasensitive and selective recognition of Hg^{2+}, and a detection limit achieved as low as 10 pM. In addition, the fluorescent biosensing system also displays remarkable specificity to Hg^{2+} against other possible competing ions. This approach was applied to the determination of real water samples with good recovery and high efficiency for practical analysis.

View Article Online
DOI: 10.1039/C8AN00377G

1. INTRODUCTION

Toxic metal such as mercury ion is a bioaccumulative and most toxic environmental pollutant with distinct toxicological profiles that can cause serious effects on human health problems. [1, 2] Even low concentration of mercury poisoning induces a wide variety of serious human diseases such as permanent damage to the nervous system, kidney damage, liver damage, brain damage, and various cognition and motion disorders.[3] Considering its toxicity, the US Environmental Protection Agency (EPA) and World Health Organization (WHO) have regulated the upper limit of Hg^{2+} levels in drinking water as 10 nM and 30 nM respectively.[4] Therefore, the development of selective and reliable detection methods for Hg^{2+} ions is a significant interest to the scientific and environmental communities.

Number of analytical methods have been developed for the accurate determination of Hg^{2+} including cold vapor atomic adsorption spectroscopy (CV-AAS),[5] electrochemical methods, cold vapor atomic fluorescence spectroscopy (CV-AFS)[6] and inductively coupled plasma mass spectroscopy (ICP-MS)[7]. Although, these conventional analytical methods require expensive and sophisticated instrumentation, professional personnel and time consuming sample pre-treatment methods, thus precluded their application for in field detection of Hg^{2+}ions. Therefore, it is an urgent need to develop a simple and sensitive method to detect Hg^{2+} ions.

In recent years, much effort has been focused on the design of DNA-based mercury ion sensor. This sensor is based on the thymine rich oligonuclotides through to form stable dsDNA with Hg^{2+} mediated (T-Hg^{2+}-T) DNA base pairing.[8-10] The binding between the Hg^{2+} ions and T-T base pair is more stable than natural adenine-thymine (A-T) base pair.[11] The development of many interesting fluorescent[12, 13] colorimetric[14, 15] and electrochemical sensor[16, 17] have been designed for Hg^{2+} using the highly specific T-Hg^{2+}-T interaction. During which, fluorescent methods have attracted great attention in various fields due to simplicity, fast response and high sensitivity. Furthermore, the target recycling amplification method is an efficient way to improve the sensitivity for detection of Hg^{2+}. To date, a variety of nucleases such as Rnase H, nicking endonuclease, endonuclease IV, exonuclease III and lambda nuclease have been employed as the cleavage enzymes to promote recycling.[18] Exo III is a kind of commonly used enzyme in target recycling amplification which can catalyze the step removal of mononucleotides successively blunt or recessed 3'-hydroxyl terminus of dsDNA.[19,20] In the view of these properties,

View Article Online
DOI: 10.1039/C8AN00377G

Exonuclease III was used as a versatile platform for highly sensitive and selective fluorescent sensor for target recycling amplification detection of Hg^{2+} ion.

Over the past few decades, various nanomaterials have been extensively applied for fluorescence detection of heavy metals and biomolecules such as gold nanoparticles, graphene oxide (GO) carbon nanotubes (CNT), MoS_2 nanosheets and metal organic frame work.[21-24] Though these nanomaterials were widely used for fluorescent biosensing methods but some of them have medium fluorescent quenching efficiency, poor biocompatibility and biodegradability, which are found to be toxic of potential application in vivo. Recently, bio-polymerized materials of polydopamine are considered to be more suitable for biological areas. The polydopamine derivatives such as polydopamine nanospheres[25], Fe_3O_4@PDA[26], PDA@$Cu_{2-x}Se$[27], PDA@CNTs[28], 2D polydopamine[29] and polydopamine nanotubes.[30] Among them, the polydopamine nanotubes are more interest due to their good biocompatibility, biodegradability and unique electrical properties. It has also been demonstrated that polydopamine nanotubes exhibit highly effective fluorescence quencher and has been broadly applied for biological applications.

We introduce a novel simple approach for sensitive and selective detection of Hg^{2+} by combination of PDNTs with Exo III assisted amplification strategy. To enhance the fluorescence intensity is using Exo III assisted amplification strategy and recycling of Hg^{2+}. To the best of our knowledge, the environmental application of polydopamine nanotubes (PDNTs) based biosensor has not been described in the previous literature. Herein, the polydopamine nanotubes mediated fluorescent biosensor for highly sensitive and selective detection of Hg^{2+} through Exo III assisted signal amplification. Furthermore, the potential application of this system for the monitoring Hg^{2+} ions in environmental samples was demonstrated.

2. EXPERIMENTAL SECTION

2.1. Materials

All synthetic oligonuclotides were ordered from integrated DNA Technologies (IDT, Avantor, India) and following sequences listed below:

View Article Online
DOI: 10.1039/C8AN00377G

Probe 1: 5'-ATGTTGTTTGTTCCCCTTCTTTCTTCTT-FAM-3'

Probe 2: 5'-GGTAAGTTCGACCCCCTCGTTCTTACC-FAM-3'

Probe 3: 5'-AACCCAGAACGCCCCCGTTCTGGGTT-FAM-3'

Tris (hydroxymethyl) aminometane, zinc acetate, PEG 400, dopamine hydrochloride, sodium hydroxide and ammonium chloride were purchased from Sigma Aldrich (India). Phenol, 4-Nitrophenol, 4-Chlorophenol, nitrobenzene, benzoic acid, mercury nitrate, lead nitrate, nickel chloride, cobalt chloride, copper chloride, cadmium chloride, iron chloride, Zinc chloride, manganese chloride and other standard chemicals are purchased from Alfa Aesar (India) and SRL chemicals PVT (India). Exonuclease III was obtained from Thermo Fisher scientific (India). 1 μM FAM-labeled ssDNA stock solutions were prepared by dissolving in Tris buffer (10 mM NaCl, 10 mM $MgCl_2$, pH= 7.5). The standard stock solution of Hg^{2+} was prepared by dissolving mercuric nitrate in ultra pure water.

2.2. Synthesis of ZnO nanorod

ZnO nanorods was synthesized according to previously reported procedure.[31] In a typical synthesis, 1.1 g $ZnAc.2H_2O$, 7.5 mL PEG400, 3 g of NaOH and 30 mL ethanol were introduced, and the mixture was followed by ultrasonication for about 30 mins at room temperature. Then the prepared mixture solution was transferred into a 50 mL Teflon-lined stainless-steel autoclave for hydrothermal treatment at 120 ºC for 12 h. Finally, the resulting product was recovered by centrifugation and washed with ethanol and it was then dried overnight in an oven at 60 ºC under a vacuum.

2.3. Synthesis of PDNTs

A polydopamine nanotube was synthesized according to the improved method.[32] To synthesis the PDNTs, first 20 mg ZnO nanorods, 20 mg dopamine hydrochloride are dissolved in 10 mL of 10 mM Tris-HCl (pH 8.5) solution. The reaction mixture was constantly agitated for 120 mins at room temperature to form ZnO@PDA hybrid nanorods followed by centrifugation and washed with distilled water for more than three times. To remove ZnO nanorods, the obtained ZnO@PDA hybrid nanorods were added into NH_4Cl aqueous solution (2M) and the suspension was stirred at 60 ºC for 30 mins. The resulting PDNTs were collected by centrifuge, washed with distilled water for more than five times and dried in vacuum at 60 ºC overnight. The prepared

View Article Online
DOI: 10.1039/C8AN00377G

PDNTs readily dispersed in water and resultant aqueous dispersion of PDNTs (7 μg/mL) was stored at room temperature.

2.4. Instrumentation

Scanning electron microcopy (SEM) images were taken on a FEI Quanta FEG 200 with an accelerating voltage of 20 kV. High resolution transmission electron microscopy (HRTEM) was performed with a JEOL, JEM, Fb-2000 instrument at accelerating voltage of 200 kV. Agilent Technologies FT-IR spectrometer (USA) is used to record the Fourier transforms infrared (FT-IR) spectra with the KBr pellet technique. The powder X-ray diffraction (XRD) pattern was obtained (PAN analytical, the Netherlands) with Cu Ka radiation at a voltage of 40 kV. The fluorescence emission spectra were performed by Fluoromax-4 Spectrofluorometer (HORIBA scientific, France). The silt width for both excitation and emission wavelength was set at 10 nm. The emission spectra were collected by exciting the samples at 200-800 nm.

2.5. Analytical procedure

The amplified detection of Hg^{2+} was investigated by 30 nM FAM-labeled T-rich ssDNA probe 1 was mixed with desired concentration of Hg^{2+} sample solution. The mixture was kept at room temperature for 10 min, followed by addition of 10 units of Exo III and Tris-HCl buffer (pH=7.5). After homogenization, the whole 200 μL solution was incubated at 37 ºC for 5 min. Then 30 μL of 7 μg/mL PDNTs solution was added in to the reaction. The mixtures were diluted to a final volume of 1 mL with Tris-HCl buffer and incubated at room temperature for 10 min before allowing fluorescence detection. The fluorescence intensity of the mixture was measured at excitation and emission wavelengths of 490 and 520 nm respectively. Each experiment was performed for three times. To investigate the selectivity of the sensing system, the fluorescence responses of 20 nM Hg^{2+} were compared with other interferential metal ions such as Ni^{2+}, Zn^{2+}, Fe^{3+}, Cu^{2+}, Ca^{2+}, Pb^{2+}, Co^{2+} and Cd^{2+} at high concentration and organic pollutants such as Phenol, 4-Nitrophenol, 4-Chlorophenol, nitrobenzene, benzoic acid.

2.6. Analysis of environmental water samples

Tap water was obtained from our laboratory. Lake water was collected from near SRM University, Potheri. In addition, the river water was taken from Tamiraparani River (Tirunelveli,

View Article Online
DOI: 10.1039/C8AN00377G

Tamil Nadu, India). Those environmental samples were filtered through a 0.22 μM membrane to remove the insoluble impurities and persistent organic pollutants. Aliquots of the environmental water samples were spiked with a stock solution of Hg^{2+} and diluted 5 times with higher concentration of Tris-HCl buffer. The fluorescence measurement of Hg^{2+} was analyzed separately by above procedure.

3. Results and discussion

3.1. Synthesis and characterization of PDNTs

Typically, ZnO nanorods were first synthesized through a solvothermal method in PEG 400 using ethanol, sodium hydroxide and zinc acetate dihydrate. Then, the ZnO nanorods were mixed with dopamine solution (10 mM Tris, pH= 8.5), the resulting in ZnO@PDA hybrid nanorods obtained by self polymerize under weak alkaline conditions. NH_4Cl aqueous solution is a removing the ZnO. Finally, the PDNTs were obtained (Fig. 1A). The morphology of the ZnO nanorods and PDNTs was characterized by SEM and TEM. The SEM image (Fig.1B) shows that the prepared ZnO nanorods were clearly observed that rod like morphology. In Fig. 1C, the successfully removed ZnO nanorods and obtained the PDNTs were observed. The HRTEM images of PDNTs in Fig.1 (D, E) shows the morphology of the tubular structure was observed after removal of ZnO nanorods. The prepared PDNTs are typical tubular structure with a smooth surface and inner diameter of the nanotubes which was measured between 40 to 50 nm with length of the tubular structure ranging from several hundred nanometers to 0.5 μm. Elemental analysis of PDNTs showed in the Fig. 1F, the important elements of carbon and nitrogen is present in the PDNTs. These results indicate that the ZnO is completely removed from PDNTS.

The powder X-ray diffraction (XRD) patterns of ZnO nanorods and PDNTs as shown in Fig. 2A. The presence of XRD pattern obtained for our synthesized ZnO nanorods and all the diffraction peaks consistent with the standard data of ZnO nanorods (JCPDS No. 36-1451). The diffraction peaks at 2θ = 31.35º, 34.52 º, 36.32 º, 47.62 º, 56.66 º, 62.77 º, 66.16 º, 68.18 º, 69.08 º and 72.47 º can be indexed to the (100), (002), (101), (102), (110), (103), (200), (112), (201) and (004) planes of ZnO nanorods respectively. After coated with PDA no additional peaks appear in the spectra. Further removal of ZnO nanorods, the characteristic peaks of ZnO disappear completely in PDNTs, indicating that fully removing ZnO nanorods and formation of PDNTs. The FT-IR

View Article Online
DOI: 10.1039/C8AN00377G

spectrum images of the prepared PDNTs are shown in Fig. 2B. The strongest broad absorption peak at 3411 cm^{-1} are associated with the stretching vibration of phenolic –OH groups. The peaks of 1628 cm^{-1} and 1512 cm^{-1} is assigned to the vibration of aromatic ring and NH groups. The peak at 1284 $cm^{-1}$is attributed to the stretching vibration of the phenolic carbon.

3.2. Design principle of the biosensor

The design principle of the fluorescent biosensor based on exonuclease assisted signal amplification method for Hg^{2+} detection is schematically illustrated in scheme 1. In the absence of Hg^{2+}, the FAM-ssDNA probe 1 adopts random coiled structure and resistant to the digestion of Exo III due to the Exo III can selectively digests the 3-terminus of dsDNA, but it has limited activity of ssDNA. The FAM-ssDNA probe 1 is easily adsorbed on the surface of PDNTs and the fluorescence signal is quenched. In the presence of Hg^{2+}, the PDNTs adsorbed FAM-ssDNA probe 1 through the formation of stable T-Hg^{2+}-T base pairing. Based on this mechanism, the Hg^{2+} in direct contact with the N3 position of thymine bases, and replaces two imino groups in the base pairing of two oppositely parallel thymine residues. The folding of the FAM-ssDNA probe 1 to form into a hairpin structure or dsDNA consisting of a 4-nt loop (CCCC) and a 12-bp stem with a blunt 3' terminus. The Exo III was activated as an enzyme, resulting in the catalyze stepwise removal of mononucleotides from the 3' terminus of the hairpin DNA, release of a Hg^{2+} from T-Hg^{2+}-T and FAM-labeled mononucleotides. The FAM labeled mononucleotides will not absorb on the PDNTs because of their less negative charge, smaller size and high diffusivity. In this way, leading to a distinct increase in the fluorescence signal would well-demonstrate the triggered activity of Exo III. Moreover, the liberating Hg^{2+} from the T-Hg^{2+}-T during digestion process and folding with new FAM-ssDNA probe 1 starts a new cycle of digestion. This catalytic cycle, trace amounts of Hg^{2+} can trigger the digestion of a large amount of FAM-ssDNA fragments and generates a great amplification fluorescence signal for ultrahigh sensitivity for the detection of very low concentrations of Hg^{2+}.

3.3. Feasibility study

For the successful design of Hg^{2+} detection amplification strategy, the optimal selection of different nucleobases with thymine containing designed DNA sequence probe. In this work, three DNA sequence probe were first selected and tested. They are: probe 1 (5'-

View Article Online
DOI: 10.1039/C8AN00377G

ATGTTGTTTGTTCCCCTTCTTTCTTCTT-FAM-3'), probe 2 (5'-GGTAAGTTCGACCCCTCTTCTGCGT-FAM-3') and probe 3 (5'-AACCCAGAACGCCCCCGTTCTGGGTT-FAM-3'). As illustrated in Fig.3A, with the addition of Hg^{2+} into solution, the highest fluorescence intensity of probe 1 was observed because probe 1 containing more number T-residue and easily interact with Hg^{2+} to form mismatch T-Hg^{2+}-T duplex structure and released from the surface of PDNTs. The probe 2 is contains only less number of thymine bases so very low fluorescence intensity is observed. Furthermore, the fluorescence intensity of probe 3 had no chance due to cytosine rich single strand DNA without T residue and could not able to form mismatch T-Hg^{2+}-T duplex structure. Therefore, this result indicate that probe 1 is finally selected by us for developing the detection of Hg^{2+} by using PDNTs with Exo III-assisted signal amplification methods.

In order to verify the validity of the proposed sensing system of Hg^{2+}, the fluorescence spectra under three different conditions were investigated and recorded. As shown in Fig.3B, the absence of Hg^{2+}, the fluorescence of FAM-ssDNA probe 1 was almost entirely quenched in the surface of PDNTs (Curve a). However, when adding Hg^{2+} the fluorescence intensity is partially recovered in presence of PDNTs. This indication is explained by weak interaction between the dsDNA and PDNTs than that between the ssDNA and PDNTs (Curve b). More importantly, upon the addition of Exo III in presence of FAM-ssDNA probe 1 and Hg^{2+}, the FAM-ssDNA probe 1 cyclically cleaved by Exo III and producing short FAM-linked mononucleotides. So the fluorescence intensity is dramatically increased and high signal-to background ratio (Curve c) is observed due to the weak affinity between the short FAM-linked mononucleotides and PDNTs. Moreover, the comparison of PDNTs with graphene oxide for fluorescence quenching performance, as showed in Fig. 3C. It is found that the fluorescence quenching efficiency of PDNTs is higher than graphene oxide. So this Exo III assisted signal amplification technique strongly indicates that highly sensitive and selective detection of Hg^{2+}.

3.4. Optimization of experimental parameters

To explore the effects of various optimization conditions on the fluorescent biosensor for Hg^{2+}, we optimize the amplification and sensing conditions including amount of Exo III, temperature, time and concentration of PDNTs. Firstly, the excessive amount of Exo III shows digestion activity is high, resulting high background signal. So amount of Exo III is an important role for

View Article Online
DOI: 10.1039/C8AN00377G

the efficient detection of Hg^{2+}. From Fig. 4A, our experimental results shows that the F/F_0 gradually increasing with an increasing amount of Exo III. However, the F/F_0 is slowly decreased with a further increasing amount of Exo III when the amount of Exo III was over 2U. Therefore, the amount of Exo III of 2U was chosen for further experimental conditions. Then, the effect of reaction temperature also plays an important role in the performance of this assay. Subsequently, we also tested the effect of temperature, from 0-60 ºC on the fluorescence sensor performance. As shown in Fig. 4B shows the fluorescence responses of the sensor at different enzymatic reaction temperatures. The F/F_0 values (F/F_0, where F_0 and F are the fluorescence signals in the absence and presence of Hg^{2+} respectively) increased rapidly as the reaction temperature rise from 20 to 40 ºC, and then decreased slightly while further increasing the temperature to 60 ºC. In order to obtain 40 ºC was employed as the optimum reaction temperature for the following experiments.

The process signal amplification was also affecting the reaction time of Exo III digestion. As shown in Fig. 4C, the F/F_0 value increased with the increasing the reaction time from 2 to 10 mins and then became stable up to 16 mins. The reason lies in that the Exo III activity was very high when the reaction time was less than 10 mins. More than 10 mins will cause the poor repeatability and unprofitable for sensitive detection of Hg^{2+}. Therefore, 10 min was considered to be the optimum reaction time. As shown in Fig. 4D, the F/F_0 value increased with increasing concentrations of PDNTs from 1 to 7 μg. After increasing the concentration of PDNTs the F/F_0 value decreased, because the short FAM labeled ssDNA fragments cleaved by Exo III was adsorbed on the excessive PDNTs. Therefore, 7 μg/mL PDNTs was chosen for optimal concentration in the further experiments. The fluorescence response to Hg^{2+} was influenced by strong acidity environment of the solution. The strong acidic solution (pH below 7.0) will reduce the affinity between the Hg^{2+} and thymine bases and disturb the solubility of DNA. On the other hand, at high pH, Hg^{2+} will form hydroxide precipitation. Therefore, the effect of pH was also investigated. As shown in Fig. 4E, the F/F_0 values were gradually increased when the pH was increased from 5 to 7.5, then decreased when the pH higher than 7.5. Thus, we consider pH 7.5 as an optimum pH.

View Article Online
DOI: 10.1039/C8AN00377G

3.5. The sensitivity towards Hg^{2+}

We then evaluated the sensitivity of proposed sensor PDNTs for Hg^{2+} under the optimized reaction conditions. As shown in Fig.5A, a dramatic increase in the fluorescence intensity was achieved with the increasing concentration of Hg^{2+} from 0 to 20 nM. As shown in Fig. 5B shows the relationship between the fluorescence intensity and different Hg^{2+} concentrations. The fluorescence intensity possesses a linear correlation to the Hg^{2+} concentration in the range from 0 to 0.1 nM (Fig. 5C), and the limit of detection (LOD) was estimated to be 10 pM according to the 3σ/slop, which was better than or comparable to some early reported fluorescence biosensor for Hg^{2+}. Therefore, the lowest detectable for proposed Hg^{2+} sensor showed an excellent sensitivity, which is comparable with these reported values of other sensor (as shown in **Table 1**) due to high efficiency of the PDNTs based Exo III - assisted signal amplification methods.

3.6. The selectivity PDNTs towards Hg^{2+}

We further examine the selectivity of the PDNTs fluorescence sensor towards Hg^{2+}, the responses of the blank solution containing 20 nM of Hg^{2+} with high concentration (5 μM) of potential interfering metal ions including Ni^{2+}, Zn^{2+}, Fe^{3+}, Cu^{2+}, Ca^{2+}, Pb^{2+}, Co^{2+} and Cd^{2+} and the fluorescence response was recorded. It was found from Fig. 5D, the Hg^{2+} could induce the significant fluorescence enhancement of the sensing system, while other metal ions did not give an observable fluorescence increase. Further to evaluate the selectivity of organic pollutants such as phenol, 4-Nitrophenol, 4-Chlorophenol, nitrobenzene, and benzoic acid with 20 nM of Hg^{2+} ions as shown in Fig. 6. The fluorescence intensity of this sensing system was monitored by separately. The fluorescent intensity of organic pollutants is very low compared to Hg^{2+}. The observation of these results shows the fluorescent sensing system exhibits high selectivity of Hg^{2+} over other competitive metal ions and organic pollutants. Apparently, the excellent selectivity of the sensing system is attributed to their strong coordination of specific T-Hg^{2+}-T base pairing and the better activity of Exo III.

3.7. Real sample Analysis

To explore the practical application of proposed sensor, it is applied to the determination of Hg^{2+} in real samples such as tap water, lake water and river water. The water samples were filtered several times before use. The samples spiked with different concentrations of Hg^{2+} were

View Article Online
DOI: 10.1039/C8AN00377G

performed using the same experimental procedure with three times. The recovery results of environmental samples are summarized in **Table 2**. It can be noted that the proposed biosensor show satisfactory results and recovery values between 94 and 105%. The finding clearly suggested that our sensing system is successfully applied to analyze Hg^{2+} in real environmental samples.

4. Conclusions

In summary, we have successfully developed polydopamine nanotubes (PDNTs) based fluorescence biosensor for the determination of Hg^{2+} with Exo III assisted signal amplification. It is based on the mechanism a small amount of Hg^{2+} can induce the large number dsDNA formation, leading to the signal amplification reaction with enhance the fluorescence signal. The detection limit of the proposed sensor is as low as 10 pM over other coexisting metal ions, which is below the maximum recommended limit in drinkable water for Hg^{2+} which is much lower than EPA (10 nM) and WHO (30 nM). The fluorescence assay was successfully applied for the determination of environmental samples with satisfactory recoveries for practical analysis. This sensing strategy have very promising account of their simple, rapid and excellent analytical performance, we believe that this fluorescence biosensor have many advantages and may find an important task in water quality monitoring for toxic metal hazard for environmental pollution.

Acknowledgements

Author acknowledges the financial support from the Department of Chemistry, SRM Institute of Science and Technology, Tamil Nadu - 603 203, India.

View Article Online
DOI: 10.1039/C8AN00377G

References

1. H. Harris, I. J. Pickering and G. N. George, Science, 2003, **301**, 1203.
2. L. Onyido, A. R. Norris and E. Buncel, Chem. Rev. 2004, **104**, 5911-5929.
3. J. Huang, X. Gao, J. Jia, J. K. Kim and Z. Li, Anal. Chem. 2014, **86**, 3209-3215.
4. M. Li, X. Zhou, W. Ding, S. Guo, N. Wu, Biosens. Bioelectron. 2013, **41**, 889-893.
5. N. Pourreza and K. Ghanemi, J. Hazard. Mater. 2010, **178**, 566-571.
6. Y. K. Li, Y. R. Xu, Y. Huang, Y. Dai, Q. F. Hu and G. Y. Yang, Chem. Asian J. 2009, **21**, 2893-2897.
7. F. X. Han, W. D. Patterson, Y. J. Xia, B. B. M. Sridhar and Y. Su, Water Air Soil Pollut. 2006, **170**, 161-171.
8. A. Ono and H. Togashi, Angew. Chem. Int. Ed, 2004, **43**, 4300-4302.
9. Y. Tanaka, S. Oda, H. Yamaguchi, Y. Kondo, C. Konjima and A. Ono, J. Am. Chem. Soc. 2007, **129**, 244-245.
10. S. Xu, L. Chen, J. Li, Y. Guan and H. Lu, J. Hazard. Mater. 2012, **237-238**, 347-354.
11. Y. Miyake, H. Togashi, M. Tashiro, H. Yamaguchi, S. Oda, M. Kudo, Y. Tanaka, Y. Kondo, R. Sawa, T. Fujimoto, T. Machina-mi and A. Ono, J. Am. Chem. Soc. 2006, **128**, 2172-2173.
12. Y. Wei, W. Zhou, Y. Xu, Y. Xiang, R. Yuan and Y. Chai, RSC. Adv. 2014, **4**, 39082-39086.
13. Y. Li, N. Liu, H. Liu, Y. Wang, Y. Hao, X. Ma, X. Li, Y. Huo, J. Lu, S. Tang, C. Wang, Y. Zhang and Z. Gao, Sci. reports, 2017, **7,** 45974.
14. T. Li, S. Dong and E. Wang, Anal. Chem., 2009, **81**, 2144-2149.
15. J. S. Lee, M. S. Han and C. A. Mirkin, Angew. Chem. Int. Ed, 2007, **46**, 4093-4096.
16. Y. Zhang, H. Zhao, Z. Wu, Y. Xue, X. Zhang, Y. He, X. Li and Z. Yuan, Biosens. Bioelectron. 2013, **48**, 180-187.
17. X. Tang, H. Liu, B. Zou, D. Tian and H. Huang, Analyst, 2012, **32**, 37-42.
18. Q. Xu, A. Cao, L. F. Zhang and C. Y. ZhangAnal. Chem. 2012, **84**, 10845-10851.
19. W. Quang, X. Wang, W. Li, X. Chen, H. Li and D. Xu, Biosens. Bioelectron. 2015, **71**, 143-149.
20. D. Fan, C. Wu, k. Wang, X. Gu, Y. Liu and E. Wang, Chem. Commun. 2016, **52**, 406-409.

View Article Online
DOI: 10.1039/C8AN00377G

21. L. Yan, H. Shi, X. He, K. Wang, J. Tang, M. Chen, X. Ye, F. Xu and Y. Lei, Anal. Chem. 2014, **86**, 9271-9277.
22. M. Zhang, H. N. Le and B. C. Ye, ACS Appl. Mater. Interfaces, 2013, **5**, 8278-8282.
23. C. Zhu, Z. Zeng, H. Li, C. Fan and H. Zhang, J. Am. Chem. Soc. 2013, **135**, 5998-6001.
24. X. Zhu, H. Zeng, X. Wei, Z. Lin, L. Guo, B. Qiu and G. Chen, Chem. Commun. 2013, **49**, 1276-1278.
25. D. Fan, C. Wu, k. Wang, X. Gu, Y. Liu, E. Wang, Chem. Commun. 2016, **52**, 406-409.
26. R. Zheng, S. Wang, T. Tian, X. Jiang, D. Fu, S. Shen, W. Yang, ACS Appl. Mater. Interfaces, 2015, **7**(29), 15876-15884
27. H. y. Zou, P. F. Gao, M. X. Gao, C. Z. Huang, Analyst, 2015, **140**, 4121-4129.
28. T. T. Zheng, R. Zhang, L. Zou, J. J. Zhu, Analyst, 2012, **137**, 1316-1318.
29. D. Hafner, L. D. Hafner, L. Ziegler, M. Lchwan, T. Zhang, M. Schneider, C. Thomas, K. Hinrichs, R. Jordan, I Amin, Adv. Mater. 2016, **28**, 1489-1494.
30. D. Fan, X. Zhu, Q. Zhai, E. Wang and S. Dong, Anal. Chem. 2016, **88**(18), 9158-9165.
31. Q. Xiang, G. Meng, Y. Zhang, J. Xu, P. Xu, Q. Pan and W. Yu, Sensors and Acuat. B-Chem. 2010, **143**, 635-640.
32. D. Yan, P. Xu, Q. Xiang, H. Mou, J. Xu, W. Wen, X. Li and Y. J. Zhang, J. Mater. Chem. A, 2016, **4**, 3487-3493.
33. G. F. Wang, G. Xu, Y. H. Zhu, X. J. Zhang, Chem. Commun. 2014, **50**, 747-750.
34. Y. Zhang, L. Tang, F. Yang, Z. Sun, Microchim Acta, 2015, **182**, 1535-1541.
35. B. Zhang, C. Wei, RSC. Adv. 2017, 7, 56289-56295.
36. J. Huang, X. Gao, J. Jia, J. K. Kim, Z. Li, Anal. Chem. 2014, **86**, 3209-3215.
37. A. Ravikumar, P. Panneerselvam, K. Radhakrishnan, Microchim Acta, 2018, **2**, 182.
38. J. R. Zhang, W. T. Huang, W. Y. Xie, T. Wen, H. Q. Luo, N. B. Li, Analyst, 2012, **137**, 3300-3305.
39. K. Srinivasan, K. Subramanian, K. Murugan, K. Dinakaran, Analyst, 2016, **141(22),** 6344-6352.
40. M. Li, Q. Y. Wang, X. D. Shi, L. A. Hornak, N. Q. Wu, Anal. Chem. 2011, **83**, 7061-7065.
41. L. B. Zhang, L. Tao, B. L. Li, L. Jing, E. K. Wang, Chem. Commun. 2010, **46**, 1476-1478.

View Article Online
DOI: 10.1039/C8AN00377G

Table of contents

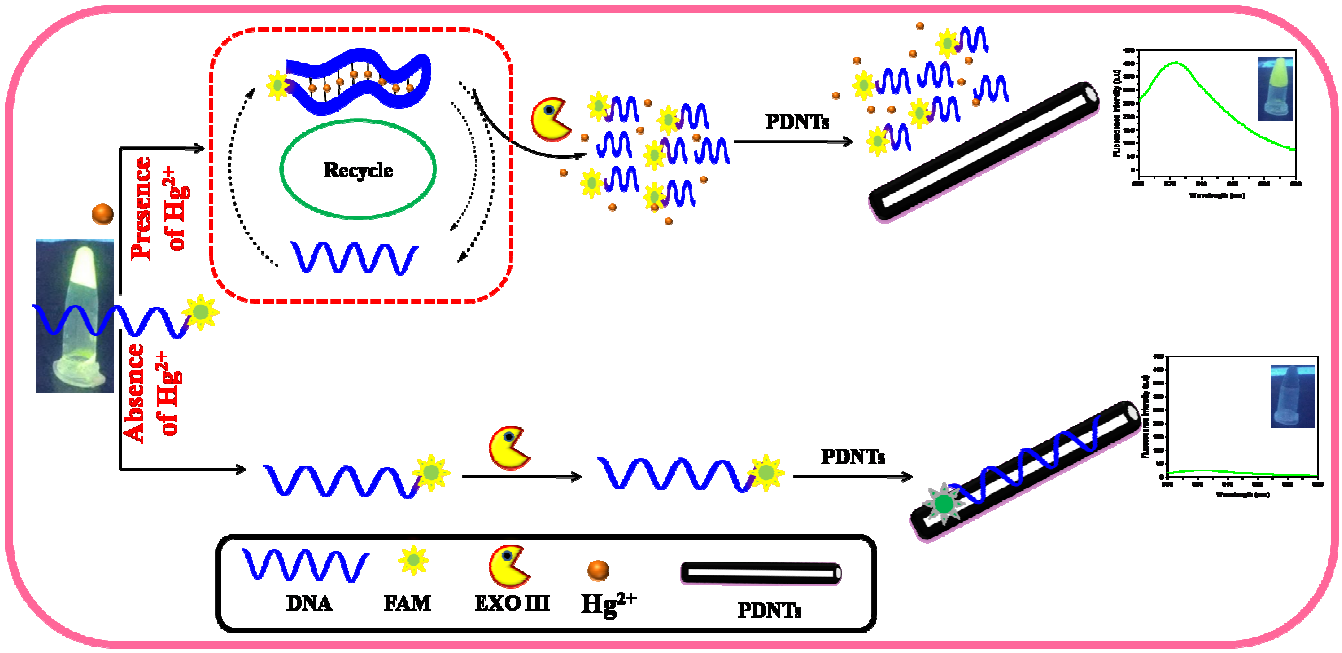

View Article Online
DOI: 10.1039/C8AN00377G

FIGURES

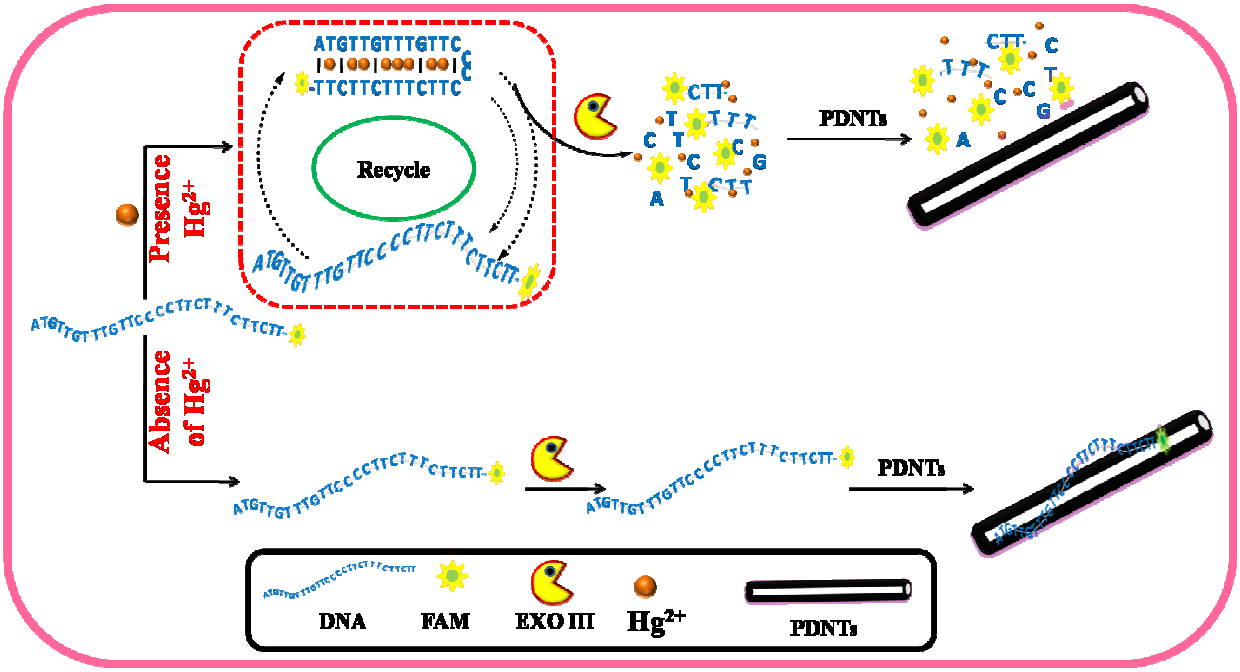

Scheme 1 Schematic illustration of fluorescence detection of Hg^{2+} by combining PDNTs with Exo III-assisted signal amplification.

View Article Online
DOI: 10.1039/C8AN00377G

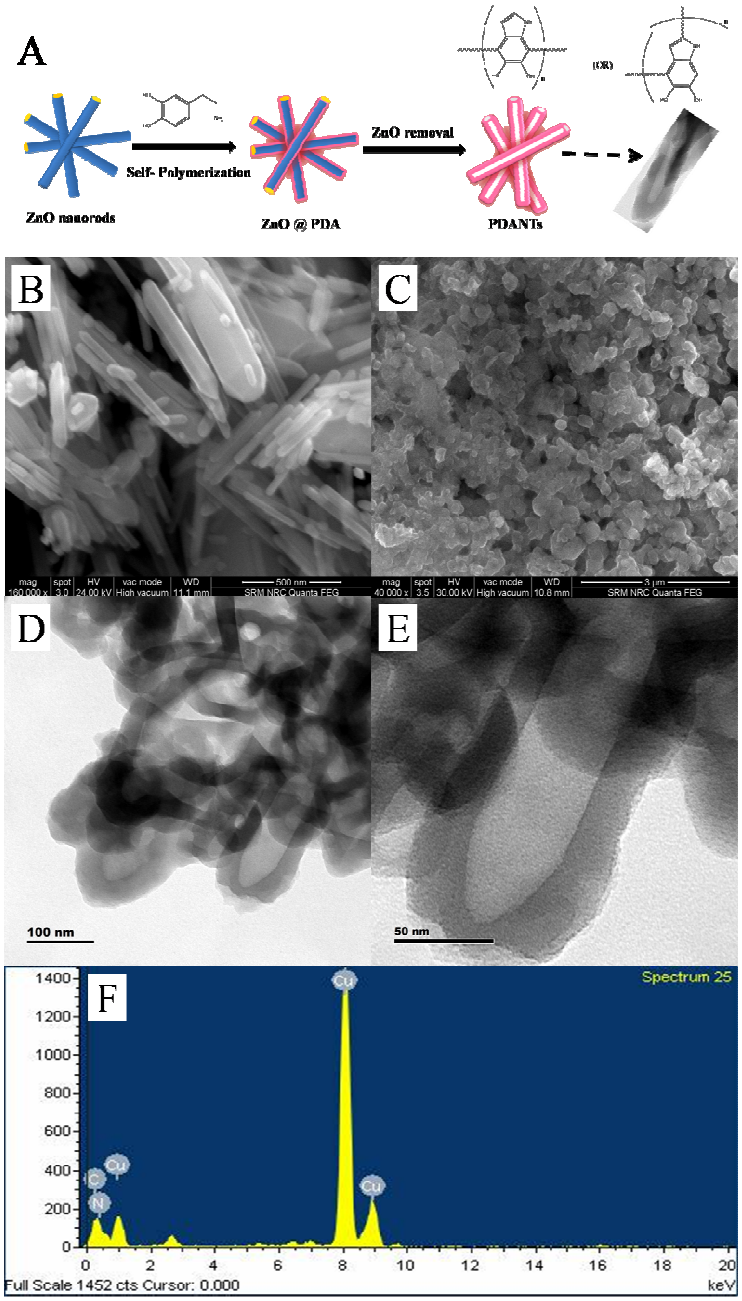

Fig. 1 (A) Scheme of synthetic route of PDNTs, (B) SEM images of ZnO nanorods and (C) PDNTs, (D, E) TEM images of PDNTs, (F) EDS spectrum of PDNTs.

View Article Online
DOI: 10.1039/C8AN00377G

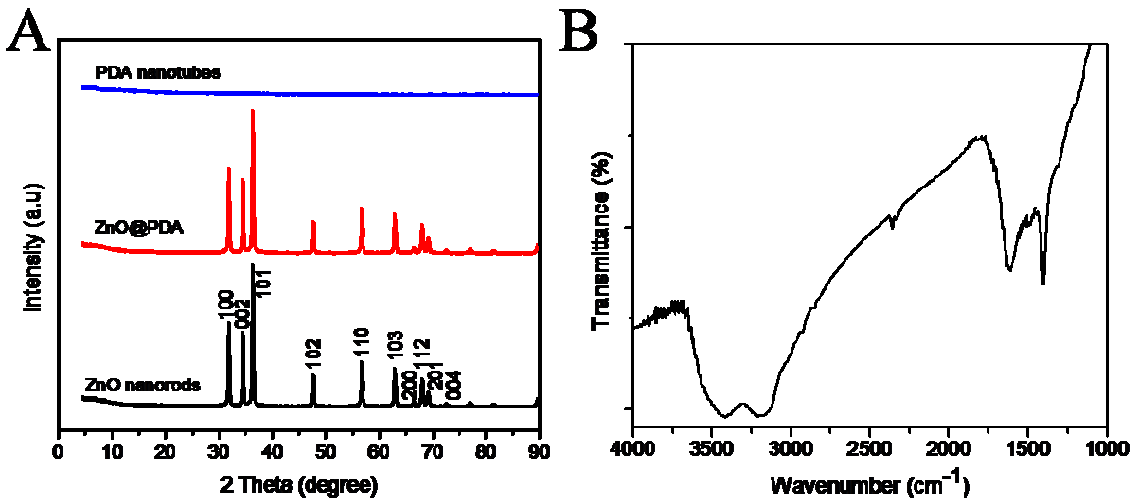

Fig. 2 The XRD patterns for (A) ZnO nanorods & PDNTs, (B) FT-IR spectra of PDNTs.

View Article Online
DOI: 10.1039/C8AN00377G

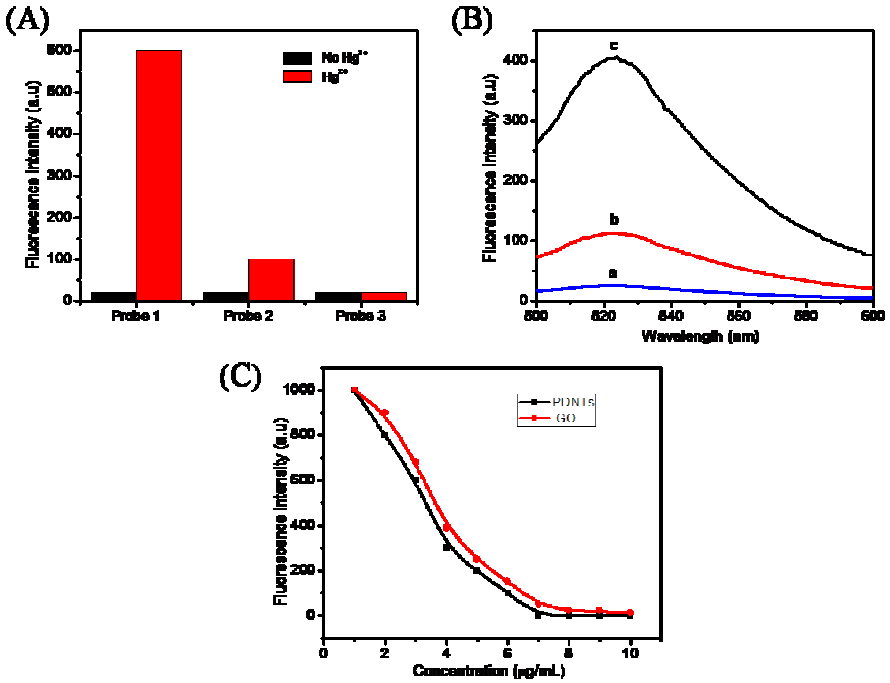

Fig. 3 (A) Fluorescence intensity of probe 1(100 nM), probe 2(100 nM) and probe 3(100 nM) in the presence (red colour) and absence (black colour) of Hg^{2+}, (B) The fluorescence spectra of Hg^{2+} detection (a) 100 nM DNA probe and 7 µg/mL PDNTs (b) 100 nM DNA probe, 7 µg/mL PDNTs and 2 U Exo III (c) 100 nM DNA probe, 7 µg/mL PDNTs, 2 U Exo III and 100 nM Hg^{2+}. (C) Fluorescence quenching assay of PDNTs verses GO. The fluorescence intensity recorded at 520 nm were obtained by gradually adding PDNTs or GO at equal concentrations in a solution of 100 nM FAM-labeled ssDNA Probe 1.

View Article Online
DOI: 10.1039/C8AN00377G

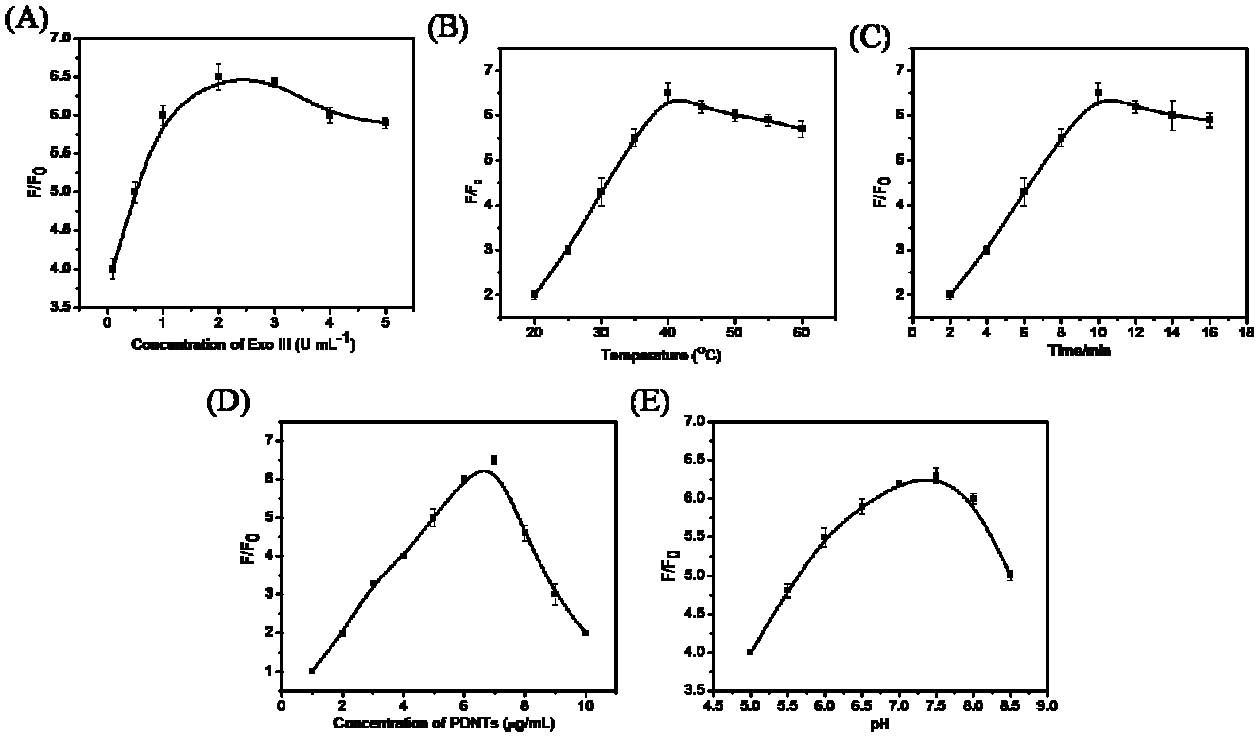

Fig. 4 Optimization of the (A) concentration of Exo III, (B) reaction temperature, (C) reaction time, (D) concentration of PDNTs, and (E) effect of pH.

View Article Online
DOI: 10.1039/C8AN00377G

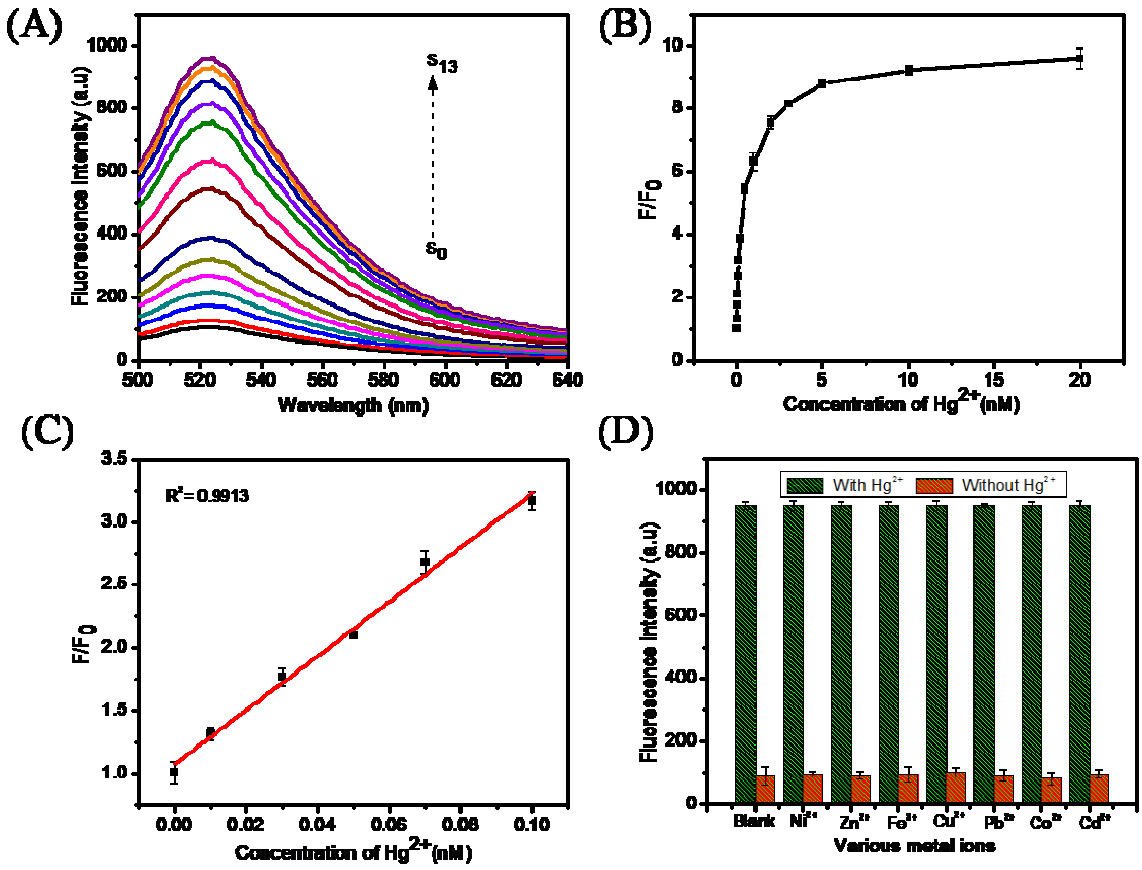

Fig. 5 (A) Typical fluorescence spectra upon the addition of different concentrations of Hg^{2+} (0 to 20 nM), (B) Fluorescence intensity versus Hg^{2+} concentrations, (C) Linear relationship between fluorescence intensity and Hg^{2+} concentrations, (D) Selectivity of the sensing method against other coexisting metal ions (Concentrations of Hg^{2+} and other metal ions were 20 nM and 5 μM respectively). Error bars are standard deviation of three experiments.

View Article Online
DOI: 10.1039/C8AN00377G

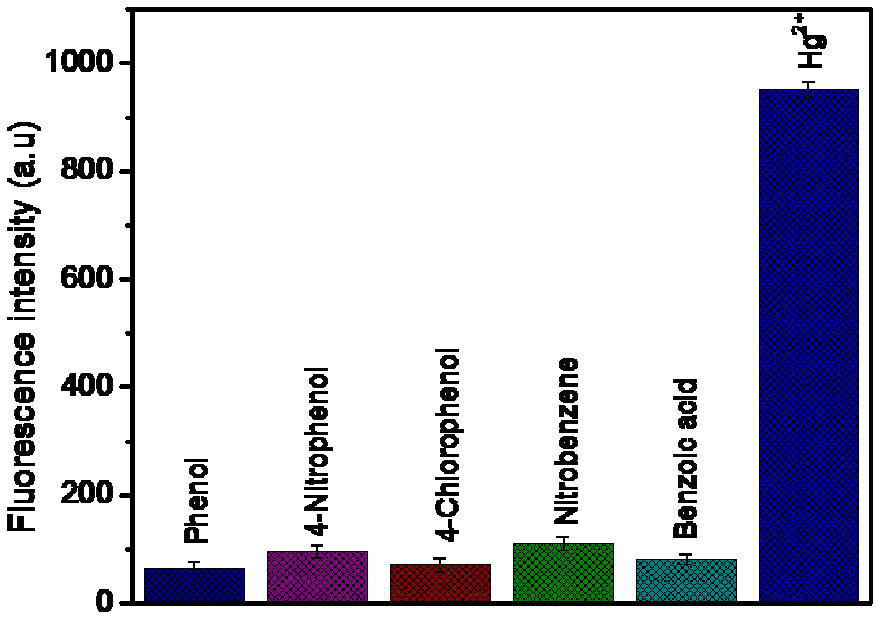

Fig. 6 Selectivity of organic pollutants with Hg^{2+} ions of this sensing system. Error bars are standard deviation of three experiments.

View Article Online
DOI: 10.1039/C8AN00377G

TABLES

Table 1 Comparison of fluorescence detection of Hg^{2+} using different nanomaterials

Materials[a]	Method[b]	Analysis time	LOD[c]	Real sample	Ref
PDNTs/Exo III	F	10 min	10 pM	Tap,lake and river water	Present work
Exo III/CNTs/AgNCs	F	160 min	33 pM	River water	33
Exo III/GO	F	8 min	0.1 nM	Lake water	34
DNA-AgNCs	F	3.5 h	0.25 nM	Lake and Tap water	35
Exo III/ GO	F	30 min	0.3 nM	Tap and river water	12
GO	F	140 min	0.3 nM	Tap water	36
GO/DNAzyme/ThT	F	40 min	356 pM	Tap and lake water	37
GO	F	10 min	0.5 nM	River water	38
MoS_2/DNA/Carbon dots	F	15 min	1.02 nM	Tap and lake water	39
QDs/Au NPs	F	10 min	2 nM	River water	40
CNTs	F	20 min	14.5 nM	Not reported	41

[a]AuNPs, gold nanoparticles; QDs, quantum dots; Exo III, exonuclease III; CNTs, carbon nanotubes; AgNCs, silver nanoclusters; GO, graphene oxide; ThT, Thioflavin; F[b] , fluorescence; LOD[c], limit of detection.

View Article Online
DOI: 10.1039/C8AN00377G

Table 2 Determination of Hg^{2+} in environmental water samples using the proposed method.

Samples	added (nM)	Found (mean[a]± [b]SD) (nM)	Recovery (%)
Tap Water 1	0	N.D	-
Tap Water 2	5	5.13± 0.15	102.6
Tap Water 3	10	9.94± 0.8	99.4
Tap Water 4	20	20.13± 0.18	100.6
Lake water 1	0	N.D	-
Lake Water 2	5	5.09± 0.11	101.8
Lake Water 3	10	10.04± 0.21	100.4
Lake Water 4	20	20.1± 0.09	100.5
River water 1	0	N.D	-
River water 2	5	4.7± 0.24	94
River water 3	10	10.5± 0.16	105
River water 4	20	19.6± 0.14	98

[a] Mean of three determinations; [b]SD Standard deviation; N.D Not detected